J. Vis. Commun. Image R. 45 (2017) 137–146

Contents lists available at ScienceDirect

J. Vis. Commun. Image R.

journal homepage: www.elsevier.com/locate/jvci

Image enhancement using divide-and-conquer strategy ☆

Peixian Zhuang, Xueyang Fu, Yue Huang, Xinghao Ding *

Fujian Key Laboratory of Sensing and Computing for Smart City, School of Information Science and Engineering, Xiamen University, China

ARTICLE INFO

Article history:
Received 15 November 2016
Revised 12 February 2017
Accepted 21 February 2017
Available online 1 March 2017

Keywords:
Image enhancement
Subspace decomposition
Gradient distribution specification
Weighted fusion

ABSTRACT

Existing enhancement methods tend to overlook the difference between image components of low-frequency and high-frequency. However, image low-frequency portions contain smooth areas occupied the majority of the image, while high-frequency components are sparser in the image. Meanwhile, the different importance of image low-frequency and high-frequency components cannot be precisely and effectively for image enhancement. Therefore, it is reasonable to deal with these components separately when designing enhancement algorithms with image subspaces. In this paper, we propose a novel divide-and-conquer strategy to decompose the observed image into four subspaces and enhance the images corresponding to each subspace individually. We employ the existing technique of gradient distribution specification for these enhancements, which has displayed promising results for image naturalization. We then reconstruct the full image using the weighted fusion of these four subspace images. Experimental results demonstrate the effectiveness of the proposed strategy in both image naturalization and details promotion.

1. Introduction

Image enhancement has been one impressive computational photography technique in image processing and computer vision [1–3]. It has been a fundamental tool for several applications, including remote sensing [4,5], biomedicine [6,7], atmospheric science [8,9] and video surveillance [10,11]. Many image enhancement techniques have been successfully developed, and can be mainly classified into the following categories:

1.1. Retinex-based algorithms

The Retinex theory assumes that color sensations strongly correlate with reflectance, and the amount of visible light reaching human eyes depends on the product of reflectance and illumination [12,13]. Retinex-based algorithms decompose an image into the illumination and the reflectance, and simultaneously compute the two components with different regularization constraints of the illumination [3,14–16]. The center/surround Retinex algorithms [17,18], such as single-scale Retinex, multi-scale Retinex and multi-scale Retinex with color restoration, used Gaussian filtering to estimate and remove the illumination, and improved image contrast and color consistency. The Retinex algorithm based on total variation adopted spatial smoothness of the illumination and piecewise continuity of the reflection [14], and used Gamma correction to compute both the illumination and the reflectance for further enhancement. A variational Bayesian Retinex approach imposed Gibbs distributions as prior distributions of the reflectance and the illumination, and employed gamma distributions for model parameters [15]. It applied variational Bayes approximation to simultaneously estimate posterior distributions of the reflectance, the illumination and hyperparameters. However, the above mentioned methods based on the Retinex theory easily suffer graying-out of uniform scenes and poorly perform in unnatural images.

1.2. Unsharp maksing techniques

The unsharp masking algorithm has been effective in image contrast and sharpness enhancement [19,20]. It focuses on using edge-preserving filters to decompose an image into a base layer and a detail layer, and processes the two parts respectively. Edge-preserving multi-scale image decompositions were presented for detail manipulation, and it used an edge-preserving smoothing operator under weighted least square framework for multi-scale detail extraction [21]. Guided filtering performed as an edge-preserving smoothing operator and displayed better behavior on image edges preservation [22]. This method generated the filtering output with the guidance of the input image or another different image. High-dimensional filtering was presented for filtering acceleration, and the resulting filter was capable of approximating standard Gaussian, bilateral, and non-local means

☆ This paper has been recommended for acceptance by Zicheng Liu.

* Corresponding author.
E-mail address: dxh@xmu.edu.cn (X. Ding).

http://dx.doi.org/10.1016/j.jvcir.2017.02.018
1047-3203/

filters [23]. These above unsharp masking algorithms favor in contrast and sharpness enhancement, but they fail in the tradeoff between details and naturalness.

1.3. Histogram equalization

Histogram equalization has been widely-used for image contrast enhancement, and it suitably adjusts the histogram of an image into a desired one. Exact histogram specification ensured the histogram of the enhanced image to be the desired uniform or brightness uniform one [24,25]. An automatic exact histogram specification technique was proposed for global and local contrast enhancement, which subjected image histogram to modification process and maximized the measure of information increase and ambiguity decrease [26]. A naturalness preserved enhancement approach was presented for image naturalness preservation, which measured the lightness-order error and used the bi-log transformation to balance details and naturalness [27]. The above mentioned methods are easily implemented but produce poor performance on image naturalness preservation. Recently, a novel algorithm based on gradient distribution specification (GDS) achieved appealing results of image naturalness, which remapped the distribution of an image to match the specified distribution learned from natural-scene image datasets [28,7]. However, this method fails in image details promotion.

It is found that existing enhancement methods tend to overlook the difference between image low-frequency and high-frequency components, and even the different importance of low-frequency and high-frequency components cannot be effectively exploited for image enhancement. Meanwhile, From Fig. 1, it is observed that the gradient distributions of four subspace images are obviously different from that of the original image, and the gradient distributions of different subspace images are also clearly different. Therefore, we develop a novel method for image enhancement using divide-and-conquer strategy. Firstly, a series of effective linear filters are designed to decompose the observed image into four subspaces. Secondly, the enhancement result of each subspace image is obtained by GDS, which is better for image naturalization. Finally, the full image is reconstructed by the weighted fusion of enhanced subspace images for details enhancement. Experimental simulations demonstrate that the proposed method outperforms other state-of-the-art methods in both naturalization and details promotion.

The paper is organized as follows: Section 2 describes the implementation of the proposed framework in detail. Experimental results are provided in Section 3 to validate the effectiveness of the proposed framework, and finally the conclusion and discussion of the paper is presented in Section 4.

2. Proposed framework

In this paper, we propose a divide-and-conquer strategy for image enhancement using subspace decomposition. We first decompose the observed image into several subspaces using linear filters, which exclusively extract either low-frequency and high-frequency information from the entire image. Then, we perform the operation of image naturalization on each of these subspace images using the method of gradient distribution specification [28]. Finally, we reconstruct the final image by fusing these subspace images with different balancing weights. It is demonstrated that image high-frequency information can be estimated more accurately under the proposed framework, which results in a more finely structured enhancement for better visual quality.

2.1. Subspace decomposition

For the desired image $\mathbf{U} \in R^{\sqrt{N}\times\sqrt{N}}$, the most direct way of image enhancement is to apply a function f to the observed image $\mathbf{I} \in R^{\sqrt{N}\times\sqrt{N}}$, i.e. $\mathbf{U} = f(\mathbf{I})$. The function f can be determined by one strategy of Retinex-based algorithms, unsharp masking techniques, and histogram equalization. Different from existing enhancement algorithms, we seek to independently enhance different frequency views of $\mathbf{U}$, called subspaces, followed by their fusion.

It is started by discussing how to find these subspaces. Let $\mathbf{h}_s$ be a predefined convolutional filter. Convolving $\mathbf{U}$ with $\mathbf{h}_s$, the s-th subspace image $\mathbf{U}_s \in R^{\sqrt{N}\times\sqrt{N}}$ is derived:

$$\mathbf{U}_s = \mathbf{U} \otimes \mathbf{h}_s \tag{1}$$

Four convolution filters are considered based on their simplicity and effectiveness. For example, using the high frequency filters $\mathbf{h}_3 = [-1, 1]$ and $\mathbf{h}_4 = [-1, 1]^T$, we obtain the subspace images $\mathbf{U}_3$

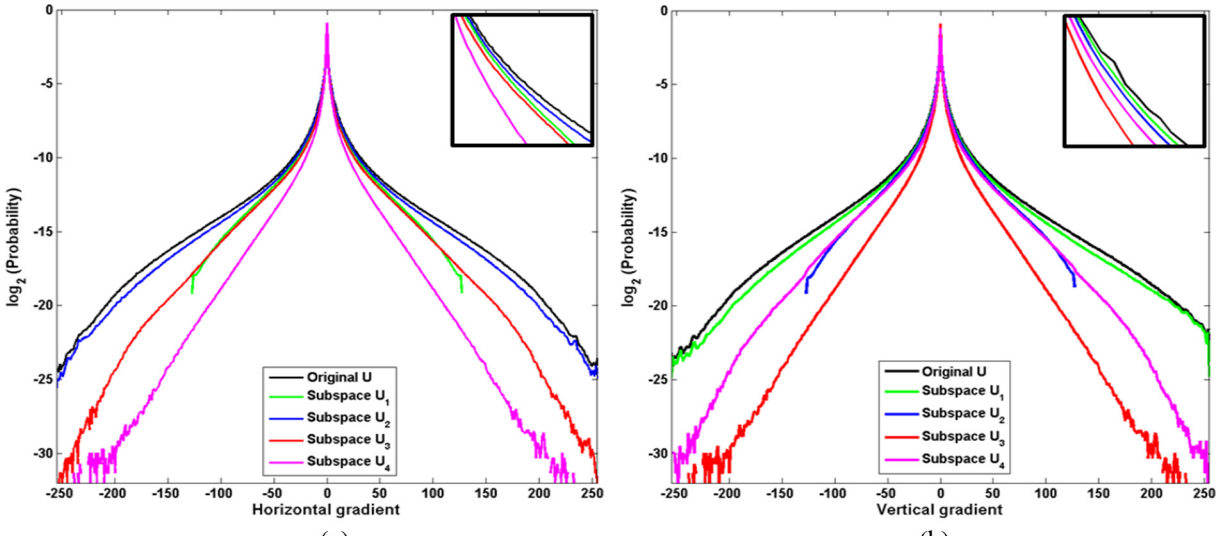

Fig. 1. Gradient distributions of original and four subspaces images. (a) and (b): average horizontal and vertical gradient distributions of 10,000 images for five kinds of images, respectively (original image $\mathbf{U}$ (black), subspace $\mathbf{U}_1 = \mathbf{h}_1 \otimes \mathbf{U}$ (green), subspace $\mathbf{U}_2 = \mathbf{h}_2 \otimes \mathbf{U}$ (blue), subspace $\mathbf{U}_3 = \mathbf{h}_3 \otimes \mathbf{U}$ (red) and subspace $\mathbf{U}_4 = \mathbf{h}_4 \otimes \mathbf{U}$ (purple); where $\{\mathbf{h}_s\}_{s=1}^4$ are defined in the Section 2.1, and the 10,000 images are from six natural-scene datasets in Table 1). (For interpretation of the references to color in this figure legend, the reader is referred to the web version of this article.)

and $\mathbf{U}_4$ that contain the high-frequency components of $\mathbf{U}$. $\otimes$ is the 2D convolution operator, and the superscript notation T is the transpose operator. We define $\mathbf{h}_1$ and $\mathbf{h}_2$ to ensure that $\mathbf{U}$ is uniquely definable in terms of $\mathbf{U}_1, \mathbf{U}_2, \mathbf{U}_3$ and $\mathbf{U}_4$. Let $\mathbf{H}_3 \in C^{\sqrt{N}\times\sqrt{N}}$ and $\mathbf{H}_4 \in C^{\sqrt{N}\times\sqrt{N}}$ be the Fourier transform of $\mathbf{h}_3$ and $\mathbf{h}_4$, respectively. Then the corresponding frequency responses of low-frequency filters are written below:

$$\mathbf{H}_1 = \mathbf{1} - \mathbf{H}_3, \mathbf{H}_2 = \mathbf{1} - \mathbf{H}_4 \tag{2}$$

where $\mathbf{1} \in C^{\sqrt{N}\times\sqrt{N}}$ is a matrix in which every element is equal to one. As a result, the above four filters are complete to ensure no information lost of the entire image during this decomposition. Based on the definition of complete filters and similar to Eq. (1), we derive the s-th observed subspace image $\mathbf{I}_s \in R^{\sqrt{N}\times\sqrt{N}}$ from the observed image $\mathbf{I}$ as

$$\mathbf{I}_s = \mathbf{I} \otimes \mathbf{h}_s \tag{3}$$

It is noted that the observed subspace images $\{\mathbf{I}_s\}_{s=1}^4$ can be obtained directly using the complete filters $\{\mathbf{h}_s\}_{s=1}^4$ to convolve the observed image $\mathbf{I}$ respectively.

2.2. Subspace enhancement

After obtaining the observed subspace image $\mathbf{I}_s$ by convolving $\mathbf{I}$ with the filter $\mathbf{h}_s$, we enhance the subspace image $\mathbf{I}_s$ independently. Based on image subspace decomposition with four filters, we treat this as four separate enhancement problems for which any enhancement algorithm can be applicable.

Table 1
Natural-scene image datasets: sources and sizes.

	Dataset	a[1]	b[2]	c[3]	d[4]	e[5]	f[6]
	Images	1005	5063	432	804	11,788	8189

[1] http://www.vision.ee.ethz.ch/showroom/zubud/.
[2] http://www.robots.ox.ac.uk/vgg/data/oxbuildings/.
[3] http://www.comp.leeds.ac.uk/scs6jwks/dataset/leedsbutterfly/.
[4] http://lear.inrialpes.fr/jegou/data.php.
[5] http://www.vision.caltech.edu/visipedia/CUB-200.html.
[6] http://www.robots.ox.ac.uk/vgg/data/flowers/102/index.html.

Table 2
Parameter selection of T_1^{pr} and T_2^{pr}.

	$\mathbf{U}_1$	$\mathbf{U}_2$	$\mathbf{U}_3$	$\mathbf{U}_4$
T_1^{pr}	0.5348	0.3352	0.8887	0.6447
T_2^{pr}	0.5361	0.3374	0.8832	0.6339

It is well-known that image enhancement with linear remapping amounts to a simple scaling of pixel intensities for standard histogram equalization, and the linear approximation accelerates the enhancement process and simplifies the algorithm. Therefore, we use the method of gradient distribution specification [28,7] to naturalize each observed subspace image separately, and reconstruct the enhanced subspace image $\mathbf{U}_s$ from linear remapping approximation:

$$\mathbf{U}_s = N_s \mathbf{I}_s \tag{4}$$

and the naturalness factor N_s is calculated by

$$N_s = (1-\theta)\frac{T_1^s}{T_1^{pr}} + \theta\frac{T_2^s}{T_2^{pr}} \tag{5}$$

where $\theta \in [0,1]$ is a balancing weight. Since the parameters of T_1 and T_2 for cumulative distribution functions of the observed image $\mathbf{I}$ are explicitly computed for any given image according to [28,7]. Specifically, for approximating the cumulative distribution functions (CDF) of image gradient, the model with the parameter T_1 is proposed as

$$\tilde{C}(\mathbf{G}) = \left(\frac{atan(T_1\mathbf{G}^x)}{\pi} + \frac{1}{2}\right)\left(\frac{atan(T_1\mathbf{G}^y)}{\pi} + \frac{1}{2}\right) \tag{6}$$

for approximating the Laplace CDF, the model with the parameter T_2 is proposed as

$$\tilde{L}(t) = \frac{atan(T_2 t)}{\pi} + \frac{1}{2} \tag{7}$$

where $\mathbf{G}^x = \mathbf{I}(x+1,y) - \mathbf{I}(x,y), \mathbf{G}^y = \mathbf{I}(x,y+1) - \mathbf{I}(x,y)$, and (x,y) is image pixel coordinate. $L(x,y) = \Delta\mathbf{I}(x,y)$, and Δ is the Laplace operator based on the second-order difference. The atan function is chosen based on the motivation of the Student-T or Cauchy distribution. Thus the subspace parameters T_1^s and T_2^s can be calculated from the observed subspace image $\mathbf{I}_s$. Furthermore, T_1^{pr} and T_2^{pr} can be learned from six datasets of natural-scene images, which are specifically shown in Table 1. Table 2 shows the respective parameters T_1^{pr} and T_2^{pr} of four subspace images, which are obtained by averaging the values over six datasets of corresponding natural-scene subspace images.

2.3. Weighted subspace fusion

Once the enhanced subspace images $\{\mathbf{U}_s\}_{s=1}^4$ are obtained, we necessarily take both the difference of subspace images and the different importance of subspace images into consideration, and effectively reconstruct the final image by the weighted fusion of

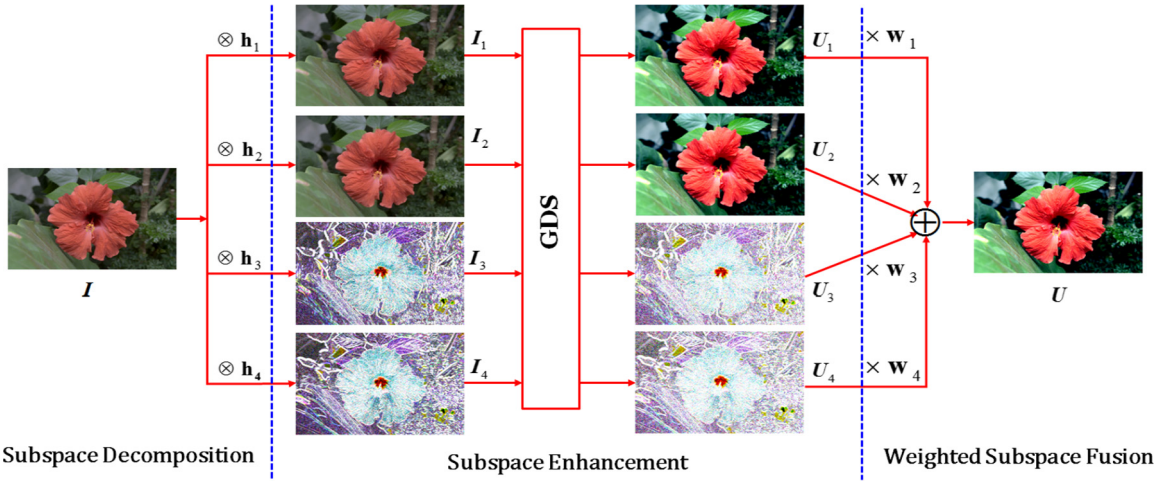

Fig. 2. Overview of proposed method.

(a) original (b) $w_1 = w_2 = 0.3$ (c) $w_1 = w_2 = 0.4$

(d) $w_1 = w_2 = 0.5$ (e) $w_1 = w_2 = 0.6$ (f) $w_1 = w_2 = 0.7$

Fig. 3. The variation of w_1 and w_2 for enhancement effect.

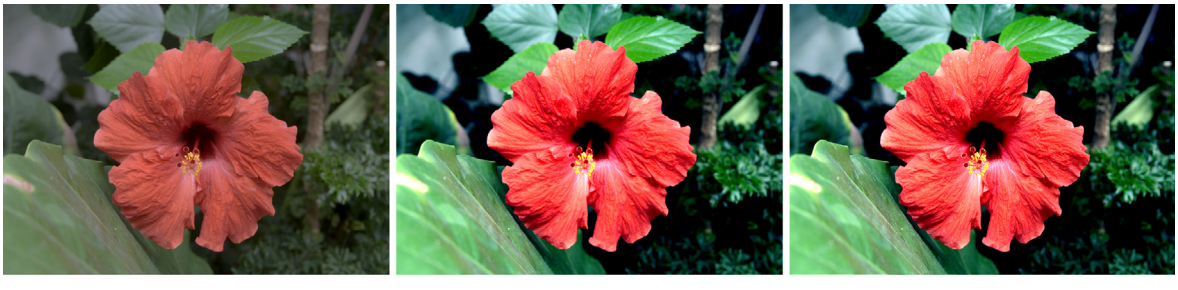

(a) original (b) $w_3 = w_4 = 0.5$ (c) $w_3 = w_4 = 1$

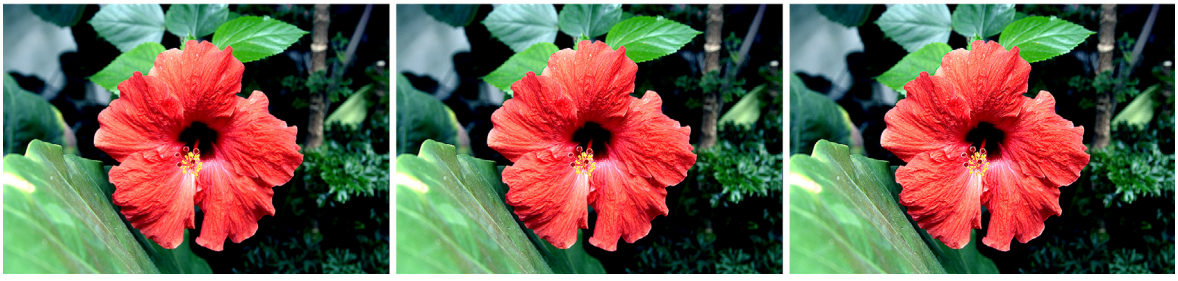

(d) $w_3 = w_4 = 1.5$ (e) $w_3 = w_4 = 2$ (f) $w_3 = w_4 = 2.5$

Fig. 4. The variation of w_3 and w_4 for enhancement effect.

these enhanced subspace images. The final solution $\mathbf{U}$ can be analytically computed:

$$\mathbf{U} = \sum_{s=1}^{4} w_s \mathbf{U}_s \tag{8}$$

where $\{w_s\}_{s=1}^4$ are the balancing weights differently adopted for different subspace images enhancement, and these weights have certain universality to be fixed for all test images.

The overview of the proposed method is shown in Fig. 2. The three main steps of the proposed method are sketched in Algorithm 1.

Algorithm 1. Outline of proposed method

Input: Observed image $\mathbf{I}$, complete filters $\{\mathbf{h}_s\}_{s=1}^4$, balancing weights $\{w_s\}_{s=1}^4$
Step 1: Generate observed subspaces $\{\mathbf{I}_s\}_{s=1}^4$ via Eq. (3);
Step 2: Obtain enhanced subspaces $\{\mathbf{U}_s\}_{s=1}^4$ via Eq. (4);
Step 3: Solve for $\mathbf{U}$ via Eq. (8).
Output: Final image $\mathbf{U}$

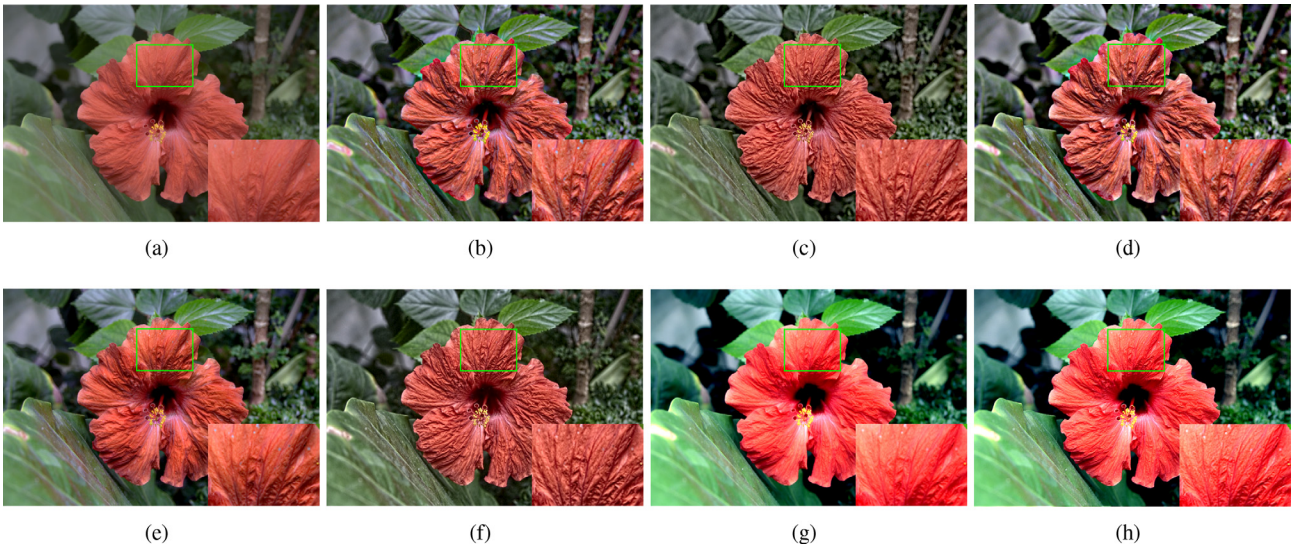

Fig. 5. Comparison of different enhancement methods on Flower image. (a) original, (b) AM [23], (c) DT [29], (d) GF [22], (e) L0 [30], (f) WLS [21], (g) GDS [28], and (h) proposed.

3. Experimental validation

In this section, we perform numerous experiments to demonstrate the effectiveness of the proposed strategy in image naturalness enhancement and details promotion. All experiments are conducted in Matlab 2012a on a SAMA computer with Intel CPU E3-1230 v3 processor (3.3 GHz) and 16 GB RAM. Each channel of color image is respectively processed by our method. The default setting of the parameter θ is 0.5 according to [28]. The enhancement effect with the variation of different weights is illustrated in Figs. 3 and 4. The balancing weights w_1 and w_2 reflect the importance of low-frequency subspaces $\mathbf{U}_1$ and $\mathbf{U}_2$ for the reconstruction

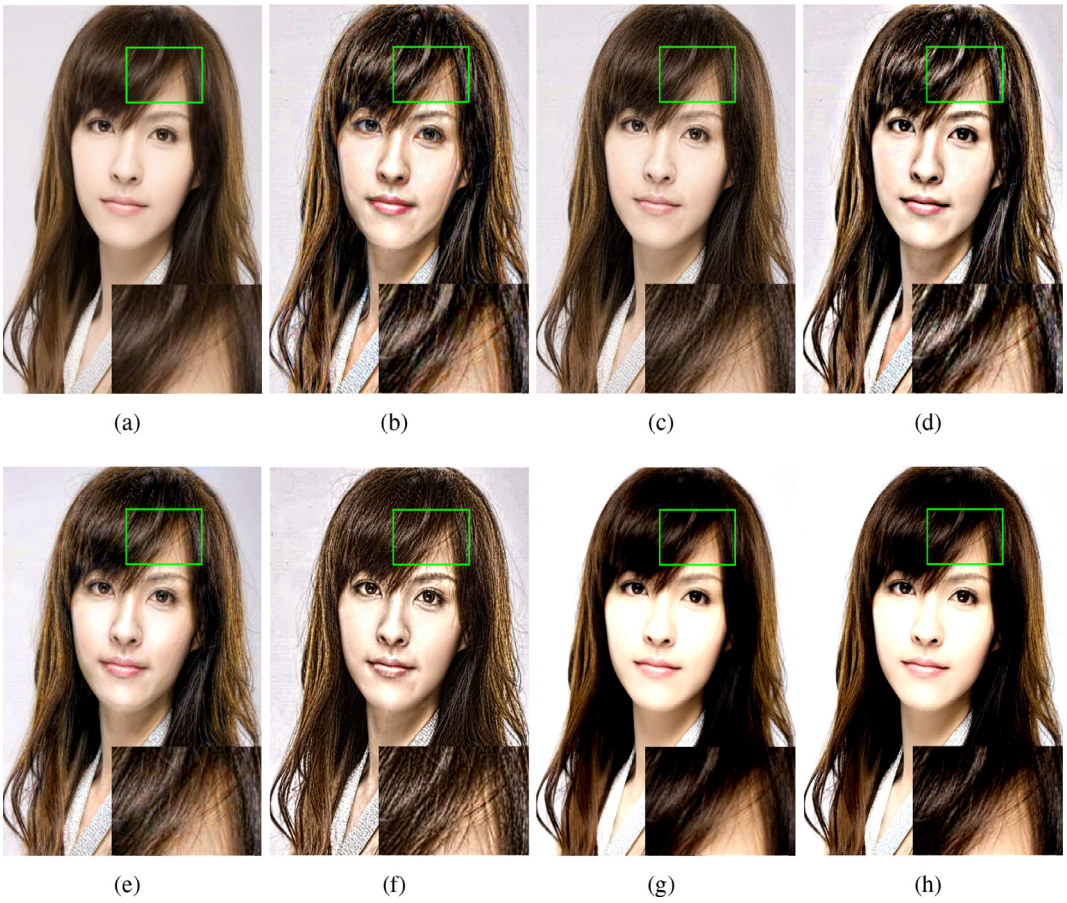

Fig. 6. Comparison of different enhancement methods on Beauty image. (a) original, (b) AM [23], (c) DT [29], (d) GF [22], (e) L0 [30], (f) WLS [21], (g) GDS [28], and (h) proposed.

of the full image **U**, while w_3 and w_4 are the weights to embody the importance of high-frequency subspaces $\mathbf{U}_3$ and $\mathbf{U}_4$. Therefore, the weights of low-frequency and high-frequency subspaces should be analyzed and set separately. Fig. 3 shows the enhancement results of the variation of w_1 and w_2 when both w_3 and w_4 are fixed to 1.5. It is seen that the brightness of the whole image becomes stronger with the increase of w_1 and w_2, and their extreme values (large or small) lead to the results of excessive brightness or excessive darkness. Therefore, we select the weight values $w_1 = w_2 = 0.5$ to be more suitable for image naturalization. Fig. 4 shows the variation of w_3 and w_4 for enhancement effect when both w_1 and w_2 are set to 0.5. It is observed that the details of the entire image becomes clearer and sharper as w_3 and w_4 increase, but the excessive enhancement result for image naturalness are generated by the weight extremum (e.g., 2.5). Therefore, we set the values of the weights w_3 and w_4 in the range of [1.5,2] for image details enhancement. We compare the proposed method against other state-of-the-art enhancement methods: Adaptive Manifolds (AM) [23], Domain Transform (DT) [29], Guided Filter (GF) [22], L0 Norm (L0) [30], Weighted Least Square (WLS) [21] and Gradient Distribution Specification (GDS) [28]. In the competing methods, the default parameter settings are used as described in the authors' papers [21–23,28–30]. For the enhancement of low illumination images, the pre-processing of Gamma correction [3] is adopted on the observed image **I**, and then all test methods are conducted on the corrected image. W and γ are empirically set 255 and 1.5, respectively.

3.1. Nature-scene and microscopy enhancement comparison

Fig. 5 shows the comparison results of different enhancement methods on image Flower, and it is clearly observed that AM [23], DT [29], GF [22], L0 [30] and WLS [21] (Fig. 5(b)–(f)) produce the enhanced results that lose image naturalness, especially

Fig. 7. Comparison of different enhancement methods on Sandstorm image. (a) original, (b) AM [23], (c) DT [29], (d) GF [22], (e) L0 [30], (f) WLS [21], (g) GDS [28], and (h) proposed.

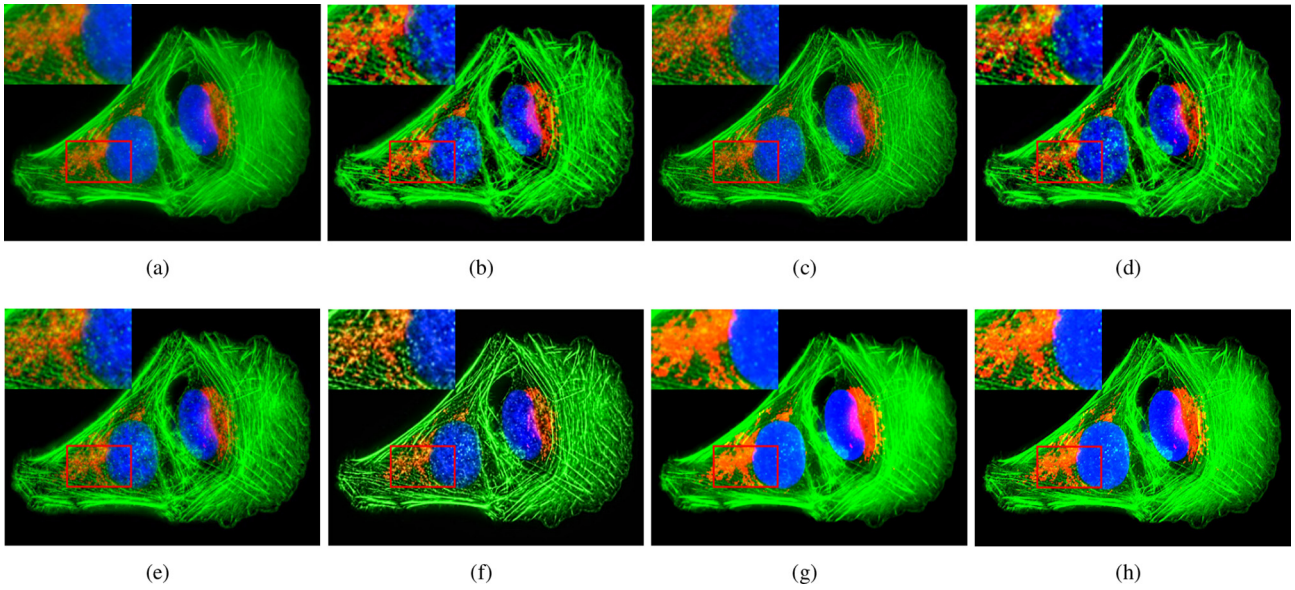

Fig. 8. Comparison of different enhancement methods on Osteosarcoma Cells image. (a) original, (b) AM [23], (c) DT [29], (d) GF [22], (e) L0 [30], (f) WLS [21], (g) GDS [28], and (h) proposed.

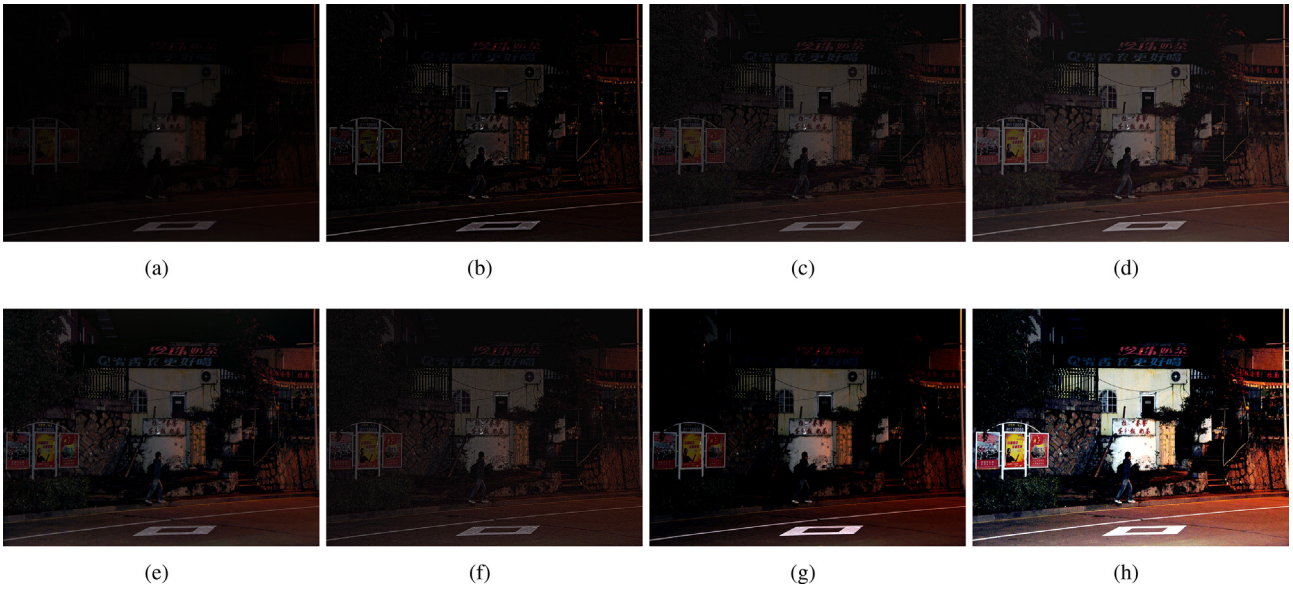

Fig. 9. Comparison of different enhancement methods on Night image. (a) original, (b) AM [23], (c) DT [29], (d) GF [22], (e) L0 [30], (f) WLS [21], (g) GDS [28], and (h) proposed.

AM [23] has serious artifacts around edges of petals and green leaves. GDS [28] (Fig. 5(g)) generates pleasing naturalization results but over-smoothes image details. However, the proposed method (Fig. 5(h)) achieves better results of naturalization and detail promotion than other methods. Some examples of poor visual quality images Beauty and Sandstorm are shown in Figs. 6 and 7 along with their enhancement results from the above mentioned enhancement algorithms. In the enhancement results of AM [23], GF [22] and L0 [30], serious artifacts are obviously produced around edges of beauty's hairs and face, woman's scarf and sweater. WLS [21] achieves clear details but with naturalness loss, DT [29] works less enhancement in image Sandstorm, and GDS [28] obtains better naturalness enhancement but fails in details promotion. In all case, it is seen that the proposed method yields more visually pleasing naturalness and clearer details than other enhancement methods, which validates the effectiveness of the proposed framework. In addition, natural-scene gradient distribution prior (GDS) [28,7] is typically applied for the enhancement of microscopy images. For the fair comparison, we perform relevant enhancement experiments on microscopy image. The results of five enhancement methods (Fig. 8(b)–(f)) are the same as above mentioned. Fig. 8(h) and (g) are the enhanced results of the proposed method and GDS [28] on Osteosarcoma Cells image. It is obviously noted that the proposed method provides better enhancement results of naturalness and details than GDS [28] that emphasizes naturalness with over-smoothed details. It is demonstrated that the proposed framework can be effectively applied for microscopy images enhancement.

3.2. Low-illumination enhancement comparison

We perform the preprocessing of Gamma correction [3] to lighten the original image, and then conduct all enhancement

Fig. 10. Comparison of different enhancement methods on Lux image. (a) original, (b) AM [23], (c) DT [29], (d) GF [22], (e) L0 [30], (f) WLS [21], (g) GDS [28], and (h) proposed.

methods on the corrected image. The enhancement results of different methods on Night and Lux images are shown in Figs. 9 and 10 respectively. We see from Fig. 9 that the results of AM [23] have serious artifacts, the results of GF [22] produce color distortion, the results obtained by DT [29] and WLS [21] introduce some noises and artifacts. L0 [30] obtains the enhancement without naturalization, and GDS [28] achieves image naturalization with details loss. However, the proposed method yields better enhancement of both naturalness and details (e.g., color and structures of Chinese characters, boy and bulletin board) than other state-of-the-art methods. From Fig. 10, it is seen that the results of color distortion are in DT [29], GF [22], L0 [30], WLS [21], serious artifacts are generated in AM [23] and WLS [21], and image details are not well enhanced in GDS [28]. However, the proposed method outperforms other methods in both naturalization and detail enhancement.

3.3. User study

In order to provide realistic feedback of users and to quantify subjective evaluation of the proposed method, we construct an independent user study, and use the enhancement results of real-world images tested in the previous section. For each test image, we randomly order the results of the seven algorithms and display them on a screen. 50 volunteers are separately participated to score each image from 1 to 5 (1 denotes the worst and 5 represents the best). From these trails, average scores of user study are shown in Table 3. This experiment offers additional support for the effectiveness of our method in the qualitative evaluation.

3.4. Enhancement comparison with weak noise

We conduct comparison experiments of different enhancement methods in different noise levels. We compare the

Table 3
Average scores of user study.

	AM [23]	DT [29]	GF [22]	L0 [30]	WLS [21]	GDS [28]	Proposed
Flower	2.55	2.86	2.61	3.90	3.14	3.71	4.07
Beauty	2.58	3.21	2.76	2.85	2.88	3.66	3.85
Sandstorm	3.09	3.60	2.77	3.29	2.93	3.50	3.67
Osteosarcoma cells	3.32	3.63	3.36	3.01	3.17	3.19	3.73
Night	2.70	3.75	3.77	3.68	3.56	3.13	3.78
Lux	2.92	3.26	3.58	4.06	2.62	3.04	4.16
Average	2.86	3.38	3.14	3.46	3.05	3.37	3.87

Fig. 11. The results of different enhancement methods in different noise levels. From left to right: (a) original, (b) GF [22], (c) AM [23] (d) GDS [28], and (e) proposed, respectively. Different rows denote different noise levels, and standard deviations of Gaussian noise from row 1 to row 5 are 0.25, 0.51, 0.76, 1.02, 1.27, respectively. **Best zoomed in on screen.**

proposed method against GF [22], AM [23] and GDS [28]. From Fig. 11, it is seen that the enhancement results of GF [22] and AM [23] are over-enhanced with naturalness loss, and some serious artifacts are generated round leaves' edges in AM [23]. The results of image naturalness are obtained by GDS [28] that incorporates natural images priors, but it places emphasis on image naturalization and fails in details enhancement. However, the proposed method obtains better naturalness and details

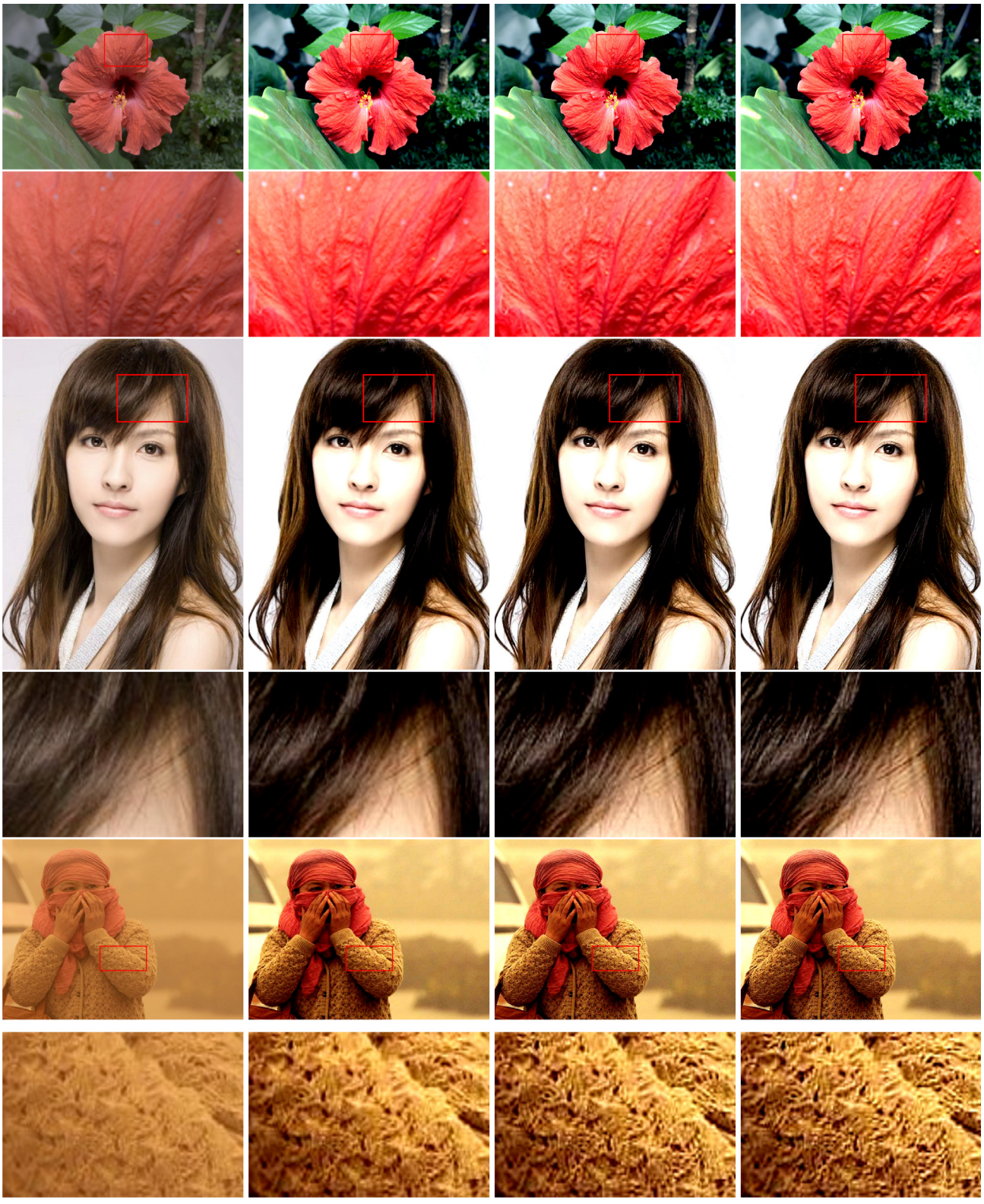

Fig. 12. Sharpening comparison of different enhancement methods. From left to right: (a) original, (b) GDS [28], (c) GDS with sharpening post-processing, and (d) proposed, respectively. **Best zoomed in on screen.**

enhancements than other methods. It is observed that the proposed method always maintains the advantages of image naturalization and details promotion in different noise levels, and it is reflected that the proposed method has certain robustness to noise.

3.5. Sharpening comparison

Image sharpening has been one useful processing technology since it brings out image details and makes edges sharper. We compare the proposed method against DGS [28] and DGS with sharpening post-processing in terms of details enhancement. In the experiment, we set both w_3 and w_4 to 2, and use the Matlab function "imsharpen" to deal with the enhanced results of GDS [28]. Fig. 12 shows the comparison results of the proposed method against GDS [28] and GDS with sharpening post-processing, and it is clearly seen that the proposed method performs better details enhancement (e.g., petal's textures, beauty's hairs and woman's sweater) than GDS [28] and GDS with sharpening post-processing. It is demonstrated that the effectiveness of the proposed framework in image details promotion.

4. Conclusion and discussion

We propose a divide-and-conquer strategy for image naturalness and details enhancements. In the proposed framework, we design effective filters to fulfill image subspace decomposition, employ GDS to enhance each subspace image for naturalness enhancement, and obtain the final image by fusing enhanced subspace images with different weights for details promotion.

We observe that the proposed framework can be more generally extended to other enhancement methods, and differently-designed filters can be easily and effectively used for image decomposition. For the limitation of the proposed method, the time consumptions of GF [22], AM [23], GDS [28] and proposed on image Flower with the size 533×800 are 0.53, 1.42, 0.85, 4.66 s, respectively. Four subspaces enhancement in the proposed framework needs higher computational costs, however, the parallel computation [31,32] by the GPU hardware can be exploited to reduce the computation time of these subspaces enhancement. These works will be explored in the near future.

Acknowledgment

This work was supported in part by the National Natural Science Foundation of China under Grants 61571382, 61571005, 81301278, 61172179, and 61103121, in part by the Guangdong Natural Science Foundation under Grant 2015A030313007, in part by the Fundamental Research Funds for the Central Universities under Grant 20720160075, 20720150169 and 20720150093, and in part by the Research Fund for the Doctoral Program of Higher Education under Grant 20120121120043.

References

[1] R. Gonzalez, R. Woods, Digital Image Processing, third ed., Prentice-Hall, Englewood Cliffs, NJ, 2007.
[2] Q. Shan, J. Jia, M.S. Brown, Globally optimized linear windowed tone-mapping, IEEE Trans. Vis. Comput. Graphics 16 (4) (2010) 663–675.
[3] X. Fu, Y. Liao, D. Zeng, Y. Huang, X. Zhang, X. Ding, A probabilistic method for image enhancement with simultaneous illumination and reflectance estimation, IEEE Trans. Image Process. 24 (12) (2015) 4965–4977.
[4] H. Demirel, C. Ozcinar, G. Anbarjafari, Satellite image contrast enhancement using discrete wavelet transform and singular value decomposition, IEEE Geosci. Remote Sens. Lett. 7 (2) (2010) 333–337.
[5] X. Fu, J. Wang, D. Zeng, Y. Huang, X. Ding, Remote sensing image enhancement using regularized-histogram equalization and DCT, IEEE Geosci. Remote Sens. Lett. 12 (11) (2015) 2301–2305.
[6] S.H. Joshi, A. Marquina, S.J. Osher, I. Dinov, J.D. Van Horn, A.W. Toga, MRI resolution enhancement using total variation regularization, in: Proceedings of IEEE International Symposium on Biomedical Imaging: From Nano to Macro, 2009, pp. 161–164.
[7] Y. Gong, I.F. Sbalzarini, A natural-scene gradient distribution prior and its application in light-microscopy image processing, IEEE J. Sel. Top. Signal Process. 10 (1) (2016) 99–114.
[8] X. Zhang, M. Constable, K.L. Chan, Aesthetic enhancement of landscape photographs as informed by paintings across depth layers, in: Proceedings of IEEE International Conference on Image Processing, 2011, pp. 1113–1116.
[9] X. Zhang, K.L. Chan, M. Constable, Atmospheric perspective effect enhancement of landscape photographs through depth-aware contrast manipulation, IEEE Trans. Multimedia 16 (3) (2014) 653–667.
[10] C. Micheloni, G.L. Foresti, Image acquisition enhancement for active video surveillance, in: Proceedings of the 17th International Conference on Pattern Recognition, 2004, pp. 326–329.
[11] Z. Jia, H. Wang, R. Caballero, Z. Xiong, J. Zhao, A. Finn, A two-step approach to see-through bad weather for surveillance video quality enhancement, in: Proceedings of IEEE International Conference on Robotics and Automation, 2011, pp. 5309–5314.
[12] E.H. Land, J.J. McCann, Lightness and the Retinex theory, J. Opt. Soc. Am. 61 (1) (1971) 1–11.
[13] M. Bertalmio, V. Caselles, E. Provenzi, Issues about retinex theory and contrast enhancement, Int. J. Comput. Vis. 83 (1) (2009) 101–119.
[14] M.K. Ng, W. Wang, A total variation model for Retinex, SIAM J. Imag. Sci. 4 (1) (2011) 345–365.
[15] L. Wang, L. Xiao, H. Liu, Z. Wei, Variational Bayesian method for Retinex, IEEE Trans. Image Process. 23 (8) (2014) 3381–3396.
[16] D. Zosso, G. Tran, S.J. Osher, Non-local Retinex-a unifying framework and beyond, SIAM J. Imag. Sci. 8 (2) (2015) 787–826.
[17] D.J. Jobson, Z.U. Rahman, G.A. Woodell, Properties and performance of a center/surround Retinex, IEEE Trans. Image Process. 6 (3) (1997) 451–462.
[18] D.J. Jobson, Z.U. Rahman, G.A. Woodell, A multiscale Retinex for bridging the gap between color images and the human observation of scenes, IEEE Trans. Image Process. 6 (7) (1997) 965–976.
[19] A. Polesel, G. Ramponi, V.J. Mathews, Image enhancement via adaptive unsharp masking, IEEE Trans. Image Process. 9 (3) (2000) 505–510.
[20] G. Deng, A generalized unsharp masking algorithm, IEEE Trans. Image Process. 20 (5) (2011) 1249–1261.
[21] Z. Farbman, R. Fattal, D. Lischinski, R. Szeliski, Edge-preserving decompositions for multi-scale tone and detail manipulation, ACM Trans. Graph. 27 (3) (2008) 67.
[22] K. He, J. Sun, X. Tang, Guided image filtering, in: Proceedings of the 11th European Conference on Computer Vision, 2010, pp. 1–14.
[23] E.S.L. Gastal, M.M. Oliveira, Adaptive manifolds for real-time high-dimensional filtering, ACM Trans. Graph. 31 (4) (2012) 33.
[24] D. Coltuc, P. Bolon, J.M. Chassery, Exact histogram specification, IEEE Trans. Image Process. 15 (5) (2006) 1143–1152.
[25] H. Ibrahim, N. Kong, Brightness preserving dynamic histogram equalization for image contrast enhancement, IEEE Trans. Consum. Electron. 53 (4) (2007) 1752–1758.
[26] D. Sen, S.K. Pal, Automatic exact histogram specification for contrast enhancement and visual system based quantitative evaluation, IEEE Trans. Image Process. 20 (5) (2011) 1211–1220.
[27] S. Wang, J. Zheng, H.M. Hu, B. Li, Naturalness preserved enhancement algorithm for non-uniform illumination images, IEEE Trans. Image Process. 22 (9) (2013) 3538–3548.
[28] Y. Gong, I.F. Sbalzarini, Image Enhancement by Gradient Distribution Specification, in: Proceedings of the 12th Asian Conference on Computer Vision, 2014, pp. 47–62.
[29] E.S.L. Gastal, M.M. Oliveira, Domain transform for edge-aware image and video processing, ACM Trans. Graph. 30 (4) (2011) 69.
[30] L. Xu, C. Lu, Y. Xu, J. Jia, Image smoothing via L0 gradient minimization, ACM Trans. Graph. 30 (6) (2011) 174.
[31] C. Yan, Y. Zhang, J. Xu, F. Dai, L. Li, Q. Dai, F. Wu, A highly parallel framework for HEVC coding unit partitioning tree decision on many-core processors, IEEE Signal Process. Lett. 21 (5) (2014) 573–576.
[32] C. Yan, Y. Zhang, J. Xu, F. Dai, J. Zhang, Q. Dai, F. Wu, Efficient parallel framework for HEVC motion estimation on many-core processors, IEEE Trans. Circ. Syst. Video Technol. 24 (12) (2014) 2077–2089.